


The stress protein heat shock cognate 70 (Hsc70) inhibits the Transient Receptor Potential Vanilloid type I (TRPV1) channel

Molecular Pain
Volume 12: 1–15
© The Author(s) 2016
Reprints and permissions:
sagepub.co.uk/journalsPermissions.nav
DOI: 10.1177/1744806916663945
mpx.sagepub.com


Mircea Iftinca, PhD, Robyn Flynn, PhD, Lilian Basso, PhD,
Helvira Melo, PhD, Reem Aboushousha, MSc, Lauren Taylor, BSc
and Christophe Altier, PhD

Abstract

Background: Specialized cellular defense mechanisms prevent damage from chemical, biological, and physical hazards. The heat shock proteins have been recognized as key chaperones that maintain cell survival against a variety of exogenous and endogenous stress signals including noxious temperature. However, the role of heat shock proteins in nociception remains poorly understood. We carried out an expression analysis of the constitutively expressed 70 kDa heat-shock cognate protein, a member of the stress-induced HSP70 family in lumbar dorsal root ganglia from a mouse model of Complete Freund's Adjuvant-induced chronic inflammatory pain. We used immunolabeling of dorsal root ganglion neurons, behavioral analysis and patch clamp electrophysiology in both dorsal root ganglion neurons and HEK cells transfected with Hsc70 and Transient Receptor Potential Channels to examine their functional interaction in heat shock stress condition.

Results: We report an increase in protein levels of Hsc70 in mouse dorsal root ganglia, 3 days post Complete Freund's Adjuvant injection in the hind paw. Immunostaining of Hsc70 was observed in most of the dorsal root ganglion neurons, including the small size nociceptors immunoreactive to the TRPV1 channel. Standard whole-cell patch-clamp technique was used to record Transient Receptor Potential Vanilloid type I current after exposure to heat shock. We found that capsaicin-evoked currents are inhibited by heat shock in dorsal root ganglion neurons and transfected HEK cells expressing Hsc70 and TRPV1. Blocking Hsc70 with matrine or spergualin compounds prevented heat shock-induced inhibition of the channel. We also found that, in contrast to TRPV1, both the cold sensor channels TRPA1 and TRPM8 were unresponsive to heat shock stress. Finally, we show that inhibition of TRPV1 depends on the ATPase activity of Hsc70 and involves the rho-associated protein kinase.

Conclusions: Our work identified Hsc70 and its ATPase activity as a central cofactor of TRPV1 channel function and points to the role of this stress protein in pain associated with neurodegenerative and/or metabolic disorders, including aging.

Keywords

transient receptor potential vanilloid type I channel, heat shock cognate 70, rho-associated protein kinase, ATPase, cell stress

Date received: 31 May 2016; revised: 4 July 2016; accepted: 11 July 2016

Background

Heat shock proteins (Hsp) belong to a large list of damage associated molecular patterns that constitute danger signals triggering inflammation and cell death. Members of the cytoplasmic 70-kDa Hsp family are critical components of the cell stress response and catalyze protein folding and trafficking. Heat-shock cognate 70 (Hsc70) is one of the four members of the Hsp70 family, with a central role in the protection of cells from damage caused by physical and chemical hazards,

Department of Physiology and Pharmacology and Snyder Institute for Chronic Diseases, University of Calgary, Calgary, Canada

Corresponding author:

Christophe Altier, Department of Physiology and Pharmacology and Snyder Institute for Chronic Diseases, University of Calgary, 3330 Hospital Dr NW, Calgary, Alberta T2N 4N1, Canada.
Email: altier@ucalgary.ca



including increasing temperature (i.e., heat shock).¹⁻³ Hsc70 is highly homologous to Hsp70; it is a constitutively and ubiquitously expressed chaperone that allows protein triage in the mammalian cytosol as well as the trafficking of ion channels.⁴ Upon stress conditions, immediate expression or oligomerization of Hsc70 will maintain cell survival and prevent apoptosis.^{3,5} Hsc70 was recently described to facilitate uncoating of clathrin-coated vesicles⁶ and mediate neurotransmitter release^{7,8} via controlling protein turnover at the synapse.⁹ It is a well characterized adenosine triphosphate (ATP) binding chaperone bearing intrinsic ATPase activity.^{1,10,11} Following ATP hydrolysis, Hsc70 binds to its substrates with high affinity in the adenosine diphosphate (ADP) bound state. Although Hsc70 was classically described to be involved in the protection of cells from stress factors, new roles for this enzyme have emerged in inflammation and aging.^{1,3,12}

The transient receptor potential vanilloid type 1 (TRPV1) channel is a polymodal calcium permeable ion channel that senses harmful physical and chemical stimuli. It belongs to the TRPV (vanilloid) subfamily that comprises six members.¹³ Each transient receptor potential (TRP) channel subtype has six identified transmembrane helices, S1–S6, with a monovalent (Na⁺, K⁺) and divalent cation (Ca²⁺) permeant pore-forming domain between S5 and S6 and intracellular amino- and carboxy-terminus regions that contain ankyrin repeats, coiled-coil domains, and calmodulin binding sites. These channels bind to interacting proteins that regulate their activity and cellular trafficking.¹⁴ Although TRPV1 are well-documented thermosensors activated by noxious heat (>42°C), they also respond to various ligands such as capsaicin, protons (H⁺), and metabolites released during inflammation^{13,15} thus highlighting their central contribution to inflammatory pain.^{16,17} Heat or reactive oxygen species produced during inflammation and tissue injury are able to activate the channel, thereby transducing nociceptive signals in primary afferent neurons.^{18,19} Given the polymodal nature of the channel and its ability to sense noxious stimuli, TRPV1 has been recognized as an important sensor of environmental stressors.²⁰⁻²²

We investigated the role of Hsc70 in the Complete Freund's Adjuvant (CFA) model of inflammatory pain and examined the possibility of a functional interaction between Hsc70 and TRPV1 channel. We report that Hsc70 is upregulated in dorsal root ganglion (DRGs) after CFA-induced paw inflammation, which coincides with the duration of hyperalgesia. We found that heat shock reduced the activity of TRPV1 channel in both native DRG neurons and transiently transfected HEK cells expressing Hsc70. We further show that a change in the ATP/ADP-bound form of Hsc70 as well as activation of the Rho effector proteins ROCK

(rho-associated protein kinase) contributes to Hsc70-mediated inhibition of TRPV1.

Methods

Plasmids

Rat TRPV1-pcDNA5/FRT and mouse TRPA1-pcDNA5/FRT were a gift from Dr. A. Patapoutian. TRPM8 was a gift from Dr R. Ramachandran. Mouse HA-Hsc70 was a gift from Dr Janice Braun. The TRPV1 point mutations S800G and S502A, to ablate phosphorylation at these residues, were generated by site-directed mutagenesis.

TRPV1-pHluorin was created by cloning a PCR-generated, ClaI site-flanked ecliptic GFP sequence into rat TRPV1-pcDNA5/FRT, using a ClaI site inserted by site-directed mutagenesis between H614 & K615, within the S5–S6 extracellular region before the re-entrant pore loop. The ecliptic GFP sequence (Ec-GFP-pcDNA3) used as PCR template was a gift from Emanuel Bourinet.

Cell culture and transient transfection

Maintenance and transfection of human embryonic kidney cells (HEK293) cells were performed as previously described.²³ Briefly, HEK cells were grown to 80% confluence at 37°C (5% CO₂) in Dulbecco's Modified Eagle's Medium (+10% fetal bovine serum (FBS), 200 units/ml penicillin and 0.2 mg/ml streptomycin (Invitrogen, Carlsbad, CA, USA)). For electrophysiology, cells were plated on glass coverslips and transfected using the calcium phosphate method with 2 µg of TRPV1, 1 µg of Hsc70, and 0.3 µg of eGFP in a 60 mm dish. Electrophysiological recordings were conducted 24 to 48 h after transfection. For biochemistry, cells were plated in a 100 mm dish and transfected with 7.5 µg of total cDNA using similar cDNA ratios.

Immunostaining and confocal microscopy

Transfected HEK cells were exposed or not to heat shock (42°C) for 1 h. After fixation in 4% PFA for 5 min, cells were incubated in blocking solution (phosphate-buffered saline, PBS + 1% BSA) for 30 min and then immunostained for 1 h at room temperature with a rabbit anti-green fluorescent protein (GFP) (Torrey Pines Scientific, Carlsbad, CA 92010). Cells were washed in PBS twice then incubated with a goat-anti rabbit IgG conjugated to Alexa Fluor 555 (Invitrogen) for 1 h. After several washes, coverslips were mounted on slides and imaged on a Zeiss 510 confocal microscope. Image analysis was conducted using ImageJ software as reported before.²⁴ Briefly, regions of interest of the plasma membrane and the intracellular compartment

were selected for each cell, then the intensity of the red signal corresponding to extracellular TRPV1 was normalized to the intensity of the green signal corresponding to total TRPV1 observed at neutral pH for pHluorin. Results were compared to the control condition (cells transfected with TRPV1 alone and cultured at 37°C.)

Dorsal root ganglia (L4–L6) were collected from CFA-injected mice and fixed for 2 h in 4% paraformaldehyde. The DRG were then embedded in OCT (Thermo-Fisher Scientific) and 8 μ m slices were cut onto Superfrost slides (VWR International, Mississauga, Ontario). The slides were washed two times in PBS and then blocked for 30 min at room temperature with a PBS solution containing 3% FBS and 0.3% Triton-X. The slides were then immunostained with anti-TRPV1 (rabbit, 1:200, Alomone Labs) and anti-Hsc70 (rat, 1:2500, Enzo Life Sciences) overnight at 4°C. Slides were washed in PBS and incubated with the Alexa-488-conjugated anti-rabbit (1:1000, Invitrogen) or Alexa-594-conjugated anti-rat (1:1000, Invitrogen) for 1 h at room temperature. Slides were washed in PBS twice and mounted with Aqua PolyMount (Polysciences Inc., Warrington, PA). Confocal images were acquired on a Zeiss LSM-510 Meta inverted microscope.

Alexa-488 antibody was visualized by excitation with an argon laser (514 nm) and emission detected using a long-pass 530 nm filter. Alexa-594 antibody was visualized by excitation at 543 nm with a HeNe laser, and emission detected using a 585–615 nm band-pass filter.

Isolation of DRG neurons

DRG neurons were excised from 6-week old mice and enzymatically dissociated in Hank's balanced salt solution (HBSS) containing 2 mg/ml collagenase and 4 mg/ml dispase (Invitrogen) for 45 min at 37°C.¹⁷ DRGs were rinsed twice in HBSS and once in culture medium consisting of Dulbecco's minimum essential medium supplemented with 10% heat-inactivated FBS, 100 μ g/ml streptomycin, 100 U/ml penicillin and 100 ng/ml Nerve Growth Factor (all from Invitrogen). Individual neurons were dispersed by trituration through a fire-polished glass Pasteur pipette in 3 ml media and cultured on glass coverslips overnight at 37°C with 5% CO₂ in 96% humidity. Coverslips were previously treated with HBSS with 25% Poly-Ornithine (Sigma) and Laminin (Sigma) at 37°C for 24 h.

Western blotting

Cells were harvested 48 h after transfection and lysed in RIPA (0.1% SDS, 1% Triton X-100, and 0.5% Na deoxycholate in PBS) with Complete EDTA-free protease inhibitor (Roche). Samples were run on tris-glycine gels

and transferred to nitrocellulose membranes, then probed with one of the following antibodies: mouse anti-HA (1:1000, Covance), rat anti-Hsc70 (1:5000, Enzo Life Sciences), or rabbit anti-VR1-N (1:1000, Neuromics), followed by an ECL-optimized HRP-conjugated secondary antibody (GE Life Sciences).

Electrophysiological measurements

For recordings, cells were placed into a 2 ml bath solution containing (in mM): 140 NaCl, 1.5 CaCl₂, 2 MgCl₂, 5 KCl, 10 HEPES, and 10 D-glucose (pH 7.4 adjusted with NaOH). Borosilicate glass (Harvard Apparatus Ltd., UK) pipettes were pulled and polished to 2–5 M Ω resistance with a DMZ-Universal Puller (Zeitz-Instruments GmbH., Martinsried, Germany). Pipettes were filled with an internal solution containing (in mM): 120 CsCl, 10 EGTA, 10 HEPES, 3 MgCl₂, 2 ATP and 0.5 GTP, pH 7.2 adjusted with CsOH. Recordings were performed using an Axopatch 200B amplifier (Axon Instruments, Foster City, CA, USA). For a subset of experiments (Figure 2(a)), CaCl₂ was removed from the bath solution. GFP-transfected cells were identified with an inverted epi-fluorescence microscope (Olympus IX51, Olympus America Inc., USA). Cells were voltage-clamped and TRPV1 currents were measured using conventional whole-cell patch clamp method. All the recordings were performed at room temperature (22 \pm 2°C) and cells (DRG and HEK) were held at V_{hold} = 0 mV in order to inactivate voltage gated Na⁺ and Ca²⁺ currents. Intracellular Cs⁺ was used to block voltage-gated K⁺ channels. In transfected HEK cells, currents were elicited by 200 ms steps between –100 mV and +100 mV at 2 s interval. Drugs were delivered using a gravitational perfusion system (ALA-VM8, Scientific Instruments) at a rate of 3–4 ml/min. In DRG neurons, during perfusion of capsaicin in the recording bath, membrane potential was held at 0 mV and currents were elicited by a ramp protocol from –100 mV to +100 mV at 1 s interval until the capsaicin-induced current reached the peak. Voltage clamp protocols were applied using pClamp 10.4 software (Axon Instruments). Data were filtered at 1 kHz (8-pole Bessel) and digitized at 10 kHz with a Digidata 1440 A converter (Axon Instruments). For whole-cell recordings, the series resistance was compensated by 65%–80%. The average cell capacitance of the DRG neurons was 16.91 \pm 1.86 pF and that of the HEK cells 24.37 \pm 1.23 pF.

For heat shock challenge, the cells were incubated at 42°C (5% CO₂) for 1 h. Only results obtained in the first 15 min after transfer from 42°C to room temperature were used. Only those cells that exhibited a stable voltage control throughout the recording were used for analysis. Because not all of the DRG neurons express TRPV1^{25–27}

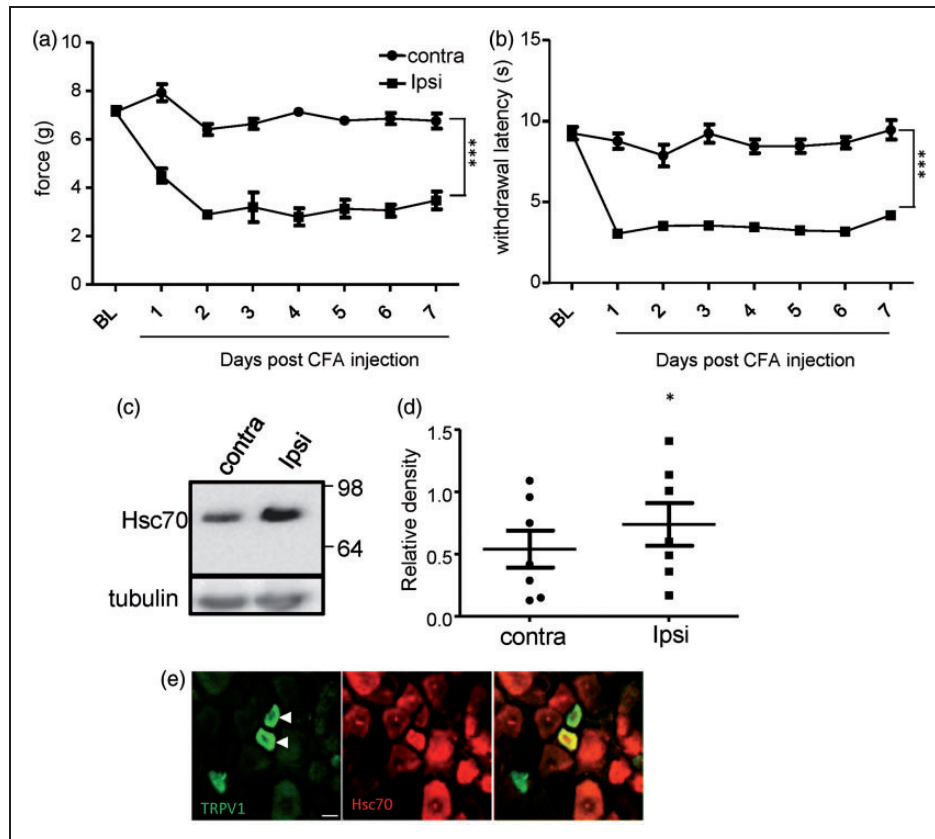


Figure 1. CFA-induced thermal and mechanical hypersensitivity coincides with an increase in Hsc70. (a) Mechanical sensitivity measured in the ipsilateral versus contralateral hind paw using the dynamic plantar aesthesiometer, before and after intraplantar injection of CFA. (b) Thermal sensitivity in the ipsilateral versus contralateral paw, measured using the Hargreaves test in mice injected with CFA. Data are expressed as mean values \pm SEM ($n=7$ mice per group); $***P < 0.001$ (two-way ANOVA analysis of variance). (c) Hsc70 protein level in DRGs (L4–L5) was increased following CFA injection in the ipsilateral paw (Ipsi) versus control (contra). (d) Densitometry analysis of Hsc70 protein level normalized to tubulin from $n=7$ mice between day 3 and 7 post CFA injection, $*P < 0.05$ (paired t test). (e) Representative immunostaining for TRPV1 (green) and Hsc70 (red) in lumbar DRG section. Note the presence of both TRPV1 and Hsc70 in small ($<20\mu\text{m}$ diameter) DRG neurons (scale bar = $20\mu\text{m}$).

only those that showed at least an 1.5-fold increase in capsaicin-induced current over the base current, elicited by a step to +100 mV, were chosen for analysis. The cells that did not show any change in the peak current were not included in the analyzed data.

Behavioral experiments

Male c57bl/6 mice aged six weeks were obtained from Charles River Canada and housed with free access to food and water, with a 12/12 light-dark cycle. All experiments were conducted on aged-matched animals, under protocols approved by the University of Calgary Animal Care Committee and in accordance with the international guidelines for the ethical use of animals in research and guidelines of the Canadian Council on Animal Care.

CFA was administered by intraplantar injection. All animals received $20\mu\text{L}$ of CFA (1 mg/ml, Sigma,

St. Louis, MO) in the right paw. The animals were assessed daily on days 1–7 after CFA injections. Prior to nociception testing, mice were habituated to the behavior room for 1 h. Mechanical threshold was assessed daily using the dynamic plantar test. Thermal sensitivity was measured using paw withdrawal latency to a radiant heat (Hargreaves apparatus from Ugo Basile). Briefly, mice on glass plates were subjected to targeted infrared heat under the ipsilateral or contralateral paw, and the paw withdrawal latency was determined by motion-sensing software. Each time point was done in triplicate. Data are presented as mean values for each group \pm SEM.

Chemicals

All drugs were obtained from Sigma with the exception of the U0126 that was purchased from Cell Signaling Technologies. Stock solutions were prepared in ethanol for menthol and mustard oil, and in dimethyl sulfoxide

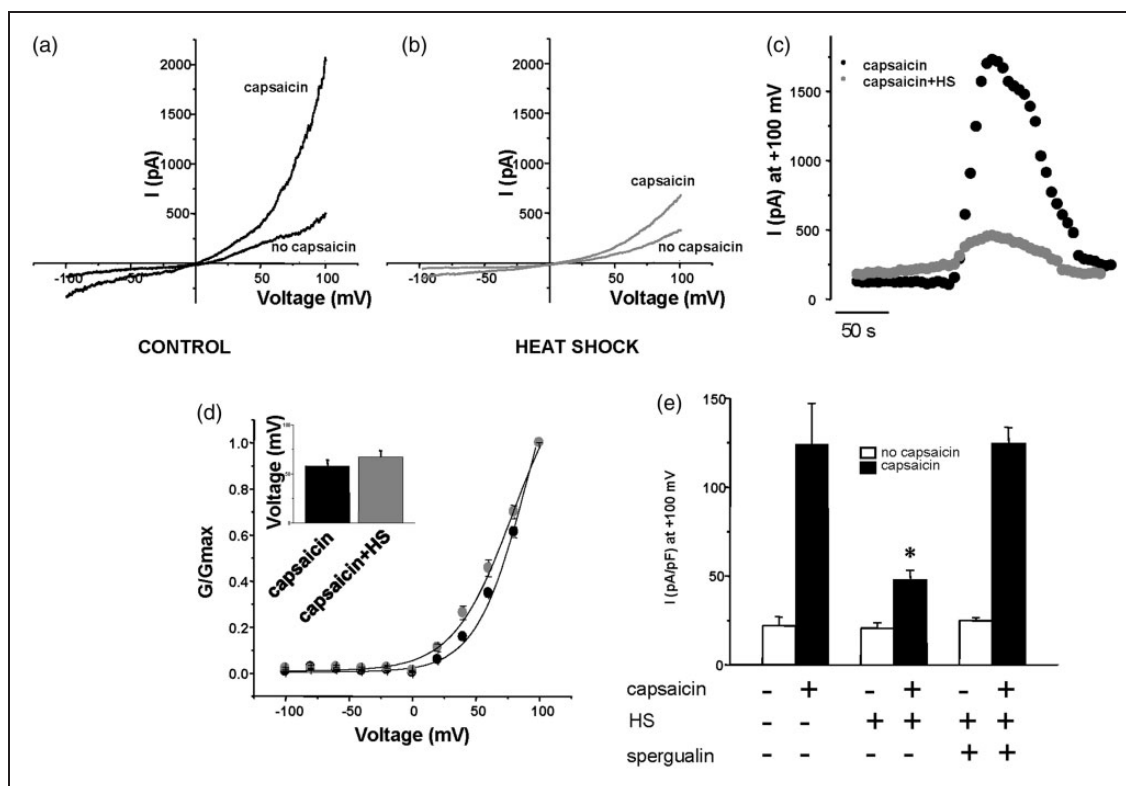


Figure 2. Effect of heat shock on capsaicin-evoked current in DRG neurons. (a) Representative whole-cell patch clamp capsaicin-induced currents recorded from a DRG neuron exposed to either 37°C (control) or 42°C (heat shock) for 1 h in calcium free solution. Voltage ramp protocol from -100 mV to $+100$ mV was applied from a holding potential of 0 mV. (b) Representative time-course of a capsaicin-evoked current in control (black) and heat shock treated (gray) DRG neurons. (c) Voltage dependence of activation (G - V curves) in the absence and presence of heat shock normalized to the respective G_{\max} values. Superimposed are best fits of a Boltzmann function with the following V_a values: 60.12 ± 5.45 ($n = 11$) vs 66.37 ± 5.93 mV ($n = 8$) (inset). (d) The Hsc70 blocker spergualin ($5 \mu\text{g/ml}$, $n = 5$) completely reverses the heat shock-induced inhibition of TRPV1 current elicited by capsaicin. Asterisks indicate a significant difference, $*P < 0.05$. Data are expressed as means \pm SEM.

(DMSO) for GFX. Neither ethanol nor DMSO had an effect on TRPA1, TRPM8, or TRPV1 current at the concentrations used (data not shown). The chemicals used in this study had the following concentrations: capsaicin 100 nM , matrine $200 \mu\text{M}$, spergualin $5 \mu\text{g/ml}$, 3-(1-[Dimethylaminopropyl]indol-3-yl)-4-[indol-3-yl]maleimide, 3-[1-[3-(dimethylamino)propyl]-1H-indol-3-yl]-4-(1H-indol-3-yl)-1H-pyrrole-2,5-dione, (GF109203X or GFX) $10 \mu\text{M}$, 1,4-diamino-2,3-dicyano-1,4-bis[2-aminophenylthio] butadiene (U0126) $10 \mu\text{M}$, (R)-(+)-trans-4-(1-Aminoethyl)-N-(4-Pyridyl)cyclohexanecarboxamide dihydrochloride (Y27632) $10 \mu\text{M}$, menthol $50 \mu\text{M}$, and mustard oil (MO) $100 \mu\text{M}$.

Statistics

Data analysis and offline leak subtraction were completed in Clampfit 10.4 (Axon Instruments), and all the curves were fitted using Origin 7.0 analysis software (OriginLab, Northampton, MA, USA).

Activation curves were fitted using the Boltzmann equation:

$$\frac{G}{G_{\max}} = \frac{1}{1 + e^{-\frac{qF}{RT}(V - V_a)/k_{act}}}$$

where G/G_{\max} is the normalized conductance estimated from the steady state current at each testing voltage, q is the equivalent gating charge, V_a is the half-activation voltage, F is the Faraday constant, T is the temperature, R is the gas constant, and k_{act} is the slope factor.

The capsaicin dose-response relationship was fitted with the Hill equation:

$$\frac{I_x - I_{\min}}{I_{\max}} = \frac{[x]^n}{EC_{50}^n + [x]^n}$$

where I_x is the steady state TRPV1 current in the presence of capsaicin at concentration $[x]$, I_{\min} , and I_{\max} are the current amplitudes in the absence and presence of a

saturating concentration of capsaicin, respectively, EC_{50} is the capsaicin concentration at which activation is half-maximal, and n is the slope factor.

All averaged data are plotted as mean \pm SEM and numbers in parentheses reflect the number of cells (n). Statistical analyses were completed with Origin 7.0 analysis software (OriginLab, Northampton, MA, USA), using paired Student's t -test for all the results obtained before and after capsaicin in the same cells, and unpaired t tests when data were obtained at the two temperatures from two separate sets of cells, and one-way analysis of variance (ANOVA) followed by the Bonferroni post hoc test for multiple comparisons. P values < 0.05 were considered statistically significant and n.s. denominates a non-significant finding.

Results

CFA induces an increase in Hsc70 protein levels in DRG neurons

To interrogate the role of HSP in pain signaling, we focused our attention on the ubiquitously and constitutively expressed member of the Hsp70 family: Hsc70, a molecular chaperone with diverse functions, including maintenance of protein homeostasis, cell survival, and autophagy.^{1,28} We asked if Hsc70 could be implicated in nociceptor sensitization that occurs during inflammation, leading to prolonged hyperalgesia and allodynia. We found that 3 to 7 days following CFA delivery, Western blot analysis in lumbar DRGs indicated an upregulation of Hsc70 that coincided with the establishment of mechanical and thermal hyperalgesia in CFA-treated mice (Figure 1(a)–(d)). Immunostaining in lumbar DRG shows Hsc70 to be abundant in neurons, including the small nociceptors expressing TRPV1 channel (Figure 3(e)).

Heat shock attenuates TRPV1 current in DRG neurons

Constitutively expressed Hsc70 was reported to be enriched in mammalian neurons where thermal cell stress triggers its translocation to synapses to preserve synaptic function.^{29,30} To determine whether HSP induction by the heat shock response could modulate ion channels in nociceptors, we examined TRPV1 channel activity by recording capsaicin-evoked currents in small DRG neurons exposed to heat shock. Cells were maintained at 42°C for 1 h in the absence of Ca^{2+} . Patch clamp recordings to assess both activity and gating of TRPV1 channels were conducted at room temperature immediately after heat shock treatment. Cells were held at 0 mV to inactivate voltage-gated Na^+ and Ca^{2+} channels while K^+ was blocked by intracellular Cs^+ (see

Methods section). As shown in Figure 2, we found an inhibition of TRPV1 currents evoked by a voltage ramp protocol (–100 to +100 mV for 200 ms) in the presence of capsaicin (Figure 2(a)) following heat shock. The peak current density obtained for a voltage step to +100 mV was significantly decreased in cells exposed to heat shock (47.52 ± 5.68 pA/pF; $n = 11$ compared to 124.14 ± 23.07 pA/pF; $n = 8$, $p < 0.05$; Figure 2(d)). Although neither the kinetics of capsaicin-induced activation (Figure 2(b)) nor the voltage dependence of the channel (Figure 2(c); V_a of 60.12 ± 5.45 vs 66.37 ± 5.93 mV) were altered by heat shock treatment, the peak current density obtained for a voltage step to +100 mV was significantly decreased in cells exposed to heat shock (47.52 ± 5.68 pA/pF; $n = 11$ compared to 124.14 ± 23.07 pA/pF; $n = 8$, $p < 0.05$; Figure 4(d)). These results suggest that Hsp induction may promote the degradation of the channel or downregulate its shuttling to the cell surface without affecting its gating. Next, we tested whether Hsc70 could mediate heat shock-induced inhibition of TRPV1 currents by treating DRG neurons with the immunosuppressive and cytostatic agent spargualin, known to block Hsc70 activity.³¹ We found that spargualin treatment restored the capsaicin-evoked current upon heat shock (Figure 2(d)), implying the contribution of Hsc70 to this effect.

Hsc70-mediated inhibition of TRPV1 channels in response to heat stress

To conduct an in-depth characterization of this regulatory process in a heterologous expression system, we verified that Hsc70-mediated inhibition could be observed with recombinant TRPV1 channels expressed in HEK cells. Patch clamp experiments were performed at room temperature following heat shock (42°C for 1 h) versus control (37° for 1 h). Typical whole cell outwardly rectifying current in response to voltage steps (–100 to +100 mV, $V_{hold} = 0$ mV) were increased to approximately six-fold from basal current in the presence of capsaicin (Figure 3(a)). However, as found with native TRPV1 channels from DRGs, exposure to heat shock significantly inhibited capsaicin-evoked current amplitude in HEK cells but only when recombinant TRPV1 channels were co-transfected with Hsc70 (Figure 3(b)), suggesting that a specific ratio of TRPV1/Hsc70 was required to mediate inhibition of exogenously overexpressed channels. In heat shocked cells, the capsaicin-induced current density at +100 mV was only a one-third of the current density measured in cells kept at 37°C (129.74 ± 9.71 pA/pF, $n = 11$ to 50.41 ± 12.20 pA/pF, $n = 8$; $p < 0.05$). Moreover, the heat shock effect was completely reversed by pretreatment with either of the Hsc70 blockers, matrine, or spargualin (peak current at +100 mV of 105.9 ± 14.67 pA/pF, $n = 5$ and

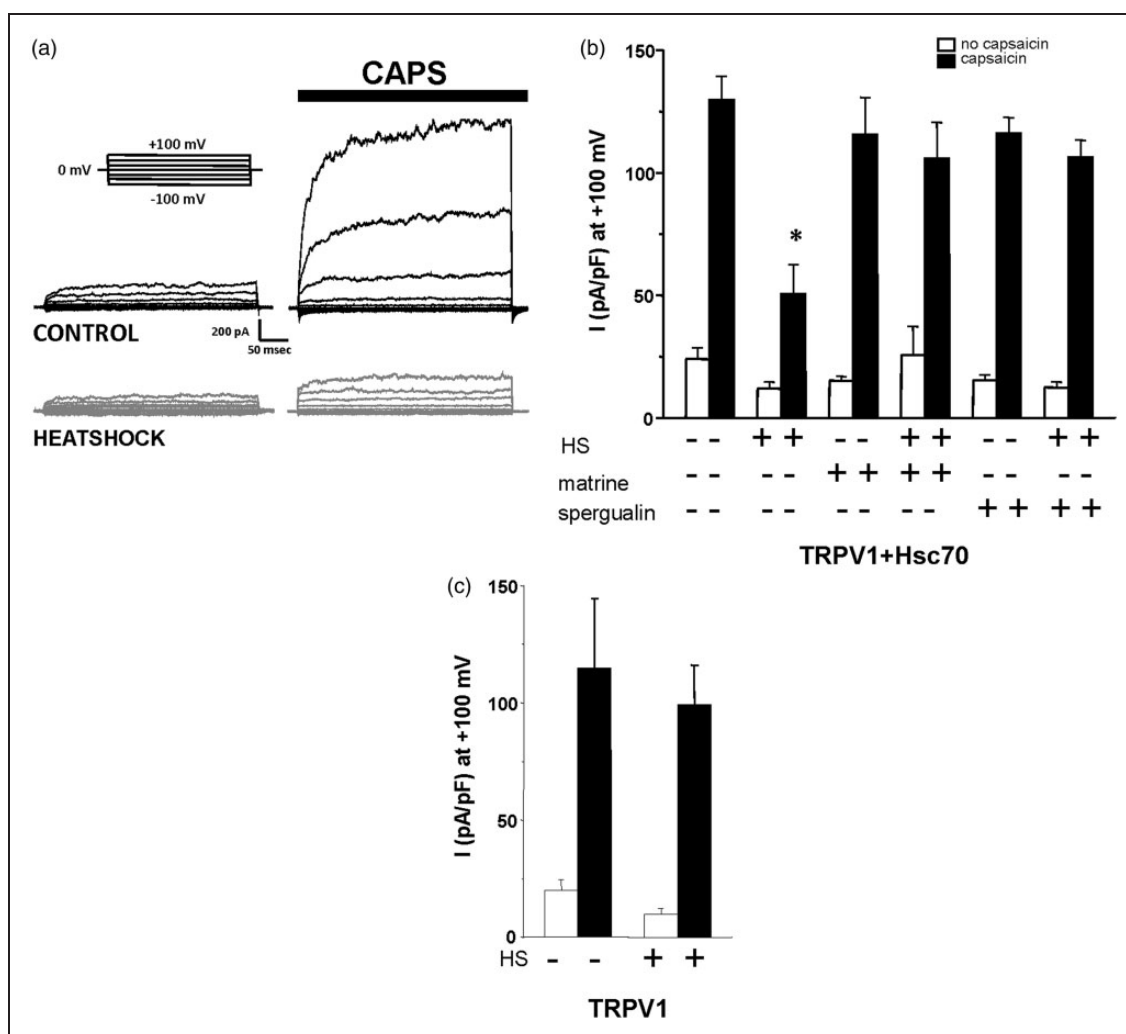


Figure 3. Heat shock inhibition of TRPV1 requires Hsc70. (a) Representative whole-cell TRPV1 current recorded from HEK cells transfected with TRPV1 and Hsc70 exposed to either 37°C (control) or 42°C (heat shock). Voltage steps were applied from a holding potential of 0 mV to various membrane potentials from -100 mV to +100 mV, in 20 mV intervals. (b) Peak capsaicin-evoked TRPV1 current density at +100 mV. The effect of heat shock is completely reversed by pretreatment with either of the Hsc70 blockers: matrine (200 μM, $n=5$) or spergualin (5 μg/ml, $n=5$) and not observed in the absence of cotransfected Hsc70 (right panel).

106.24 ± 7.11, $n=5$, respectively), confirming that activity Hsc70 ATPase activity of the chaperone preserves TRPV1 channel function, a process altered during heat shock (Figure 3(b)). Next, we queried the mechanism by which Hsc70 can inhibit capsaicin-induced current; could it result from channel desensitization triggered by a shift in the temperature sensitivity of TRPV1? We first assessed the $T_{1/2}$ (temperature of half maximal conductance) of the channel and found identical $T_{1/2}$ in absence (37.34 ± 4.02°C) or presence (35.44 ± 3.23°C) of Hsc70 ($n=4$ for each point, Figure 4(a)), indicating that Hsc70 does not alter the temperature sensitivity of the channel. We then measured channel desensitization by analyzing the effect of repeated capsaicin stimulation in calcium-free

solution following heat shock condition. Desensitization to capsaicin had a similar pattern upon repeated applications of capsaicin (100 nM) with or without heat shock treatment (Figure 4(b)), and quantification of channel desensitization was similar regardless of the temperature the cells were exposed to (Figure 4(c)), indicating that TRPV1 desensitization does not play a role in current inhibition.

We also examined whether Hsc70-mediated inhibition was due to an alteration in the voltage dependence or capsaicin sensitivity of the channel (Figure 5). As described in DRGs, we found no significant difference in the V_a from heat shocked versus control cells expressing TRPV1 and Hsc70 (65.54 ± 5.41 mV; 67.15 ± 6.34 mV; Figure 5(a)). Although the heat shock

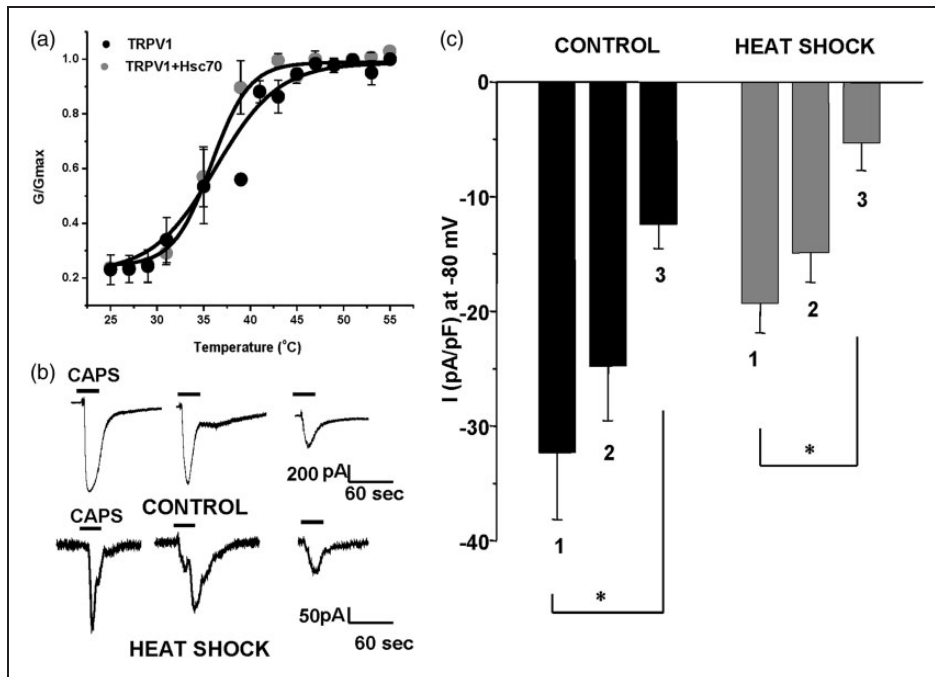


Figure 4. Desensitization of TRPV1 current is unchanged by heat shock. (a) Conductance–temperature relationship in HEK cells transfected with TRPV1 (black) or TRPV1 + Hsc70 (gray) ($n = 4$ for each data point). (b) Sample recording responses to three consecutive applications of capsaicin (100 nM, 20 sec) separated by a 5 min wash in HEK cells expressing TRPV1 and Hsc70 at a holding potential of -80 mV. (c) Histogram representing the peak of TRPV1 current density obtained at -80 mV for each of the three consecutive applications of capsaicin (100 nM) in control and heat shock condition. Data are expressed as means \pm SEM. $n = 5$ for each column. * $P < 0.05$. One way ANOVA followed by the Bonferroni post hoc test.

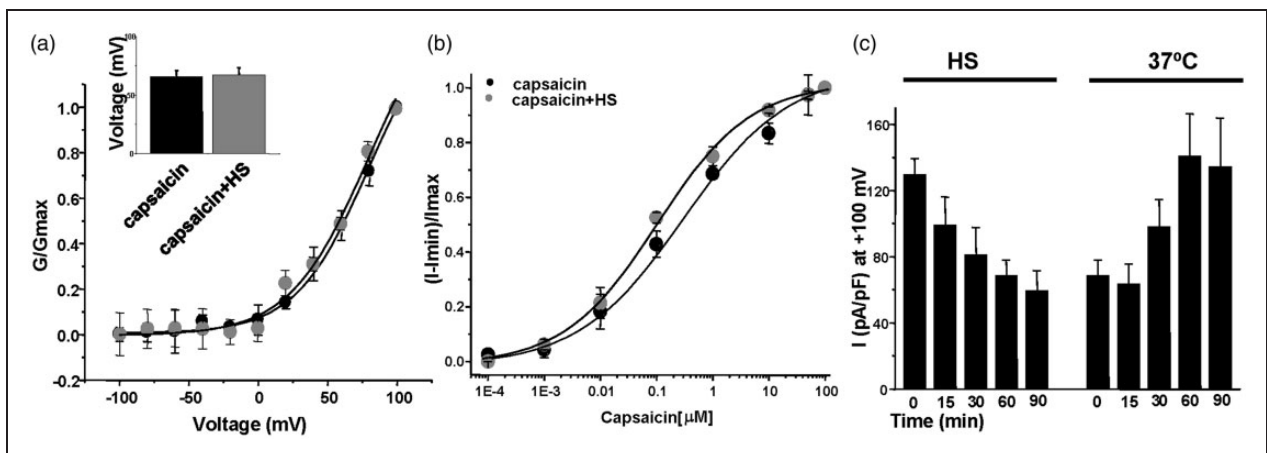


Figure 5. Voltage and capsaicin sensitivity of TRPV1 upon heat shock treatment. (a) Voltage dependence of TRPV1 activation (G-V) in capsaicin-stimulated HEK cells cotransfected with TRPV1 and Hsc70 in the absence (black) and presence (gray) of heat shock. Superimposed are best fits of a Boltzmann function and the $V_{1/2}$ values are: 65.54 ± 5.41 mV ($n = 11$) and 67.15 ± 6.34 mV without (black) and with (gray) heat shock, respectively ($n = 8$). (b) Capsaicin dose-response curves from HEK cells cotransfected with TRPV1 and Hsc70 with (gray) or without (black) heat shock ($n = 5$ for each data point). Curves represent fits of a Hill equation. (c) Time-course of the capsaicin-evoked peak current density at $+100$ mV, recorded during and after exposure to heat shock ($n = 6$ for each column). Data are expressed as mean values \pm SEM.

exposure slightly altered the capsaicin EC50 ($0.11 \pm 0.05 \mu\text{M}$ after heat shock vs $0.38 \pm 0.05 \mu\text{M}$ before), the Hill slope factor was similar in both cases (2.69 ± 0.07 and 2.05 ± 0.07 , $n=5$ for each point; Figure 5(b)). It was interesting to note that regulation of TRPV1 by Hsc70 was a dynamic process since we were able to reverse the inhibition by returning cells to physiological temperature (37°C) for 1 h after heat shock (peak current density at $+100\text{mV}$ of $140.97 \pm 25.48 \text{ pA/pF}$ compared to the peak current of 129.74 ± 9.7 in the absence of heat shock, $n=4$) (Figure 5(c)). Overall, our results suggest that heat shock-induced inhibition of TRPV1 current is not mediated by a desensitization of the channel, a change in voltage sensitivity, or a reduced affinity of the channel for capsaicin, and channel degradation is unlikely due to the short recovery period. Finally, we asked whether current inhibition could be

explained by a rapid degradation of the channel or its removal from the cell surface. As shown in Figure 6(a), we found no change in total TRPV1 protein level in Hsc70-transfected cells before and after heat shock. However, analysis of surface expressed channel using a TRPV1 tagged with an extracellular pHluorin moiety denoted a pronounced reduction in the fraction of membrane-localized channels after heat shock treatment in Hsc70-transfected cells, whereas channel removal did not occur in cells expressing TRPV1 only (Figure 6(a) and (c)), suggesting that TRPV1 channels are internalized in response to heat shock.

To determine if the heat shock-mediated inhibition was a general mechanism of endocytosis that affect most membrane-bound ion channels, we measured the heat shock modulation of exogenously expressed TRPA1 or TRPM8 channels in Hsc70-transfected cells.

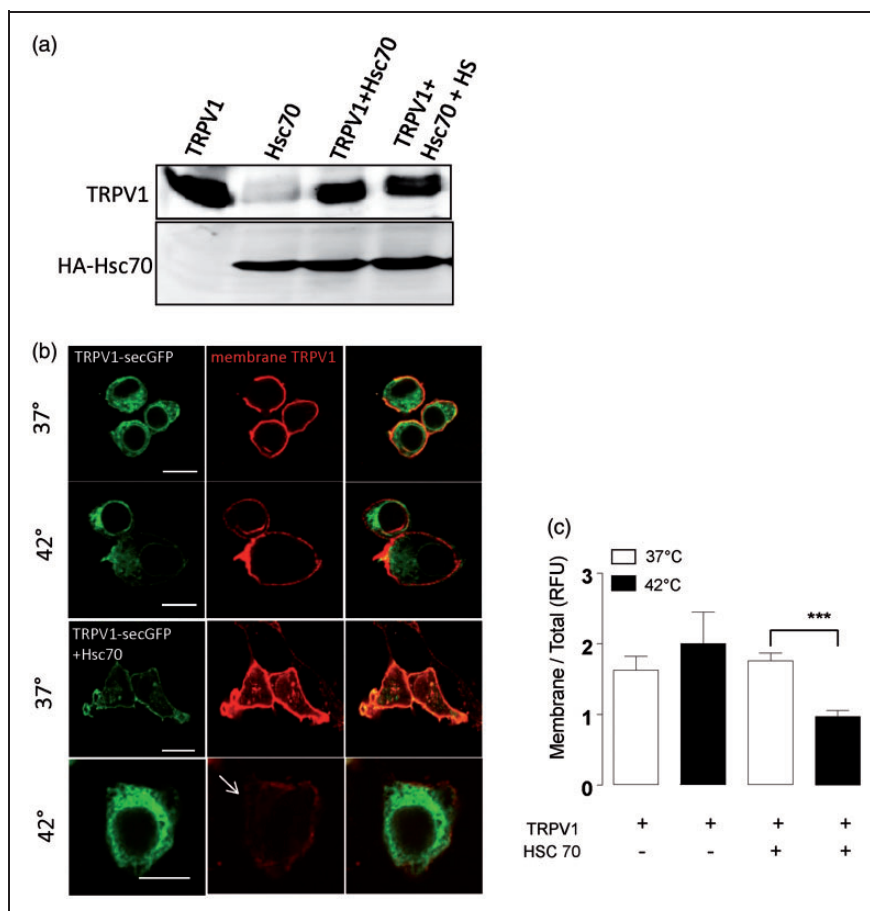


Figure 6. Hsc70-mediated TRPV1 current inhibition occurs via suppression of TRPV1 channel incorporation at the cell surface. (a) Western blot analysis of TRPV1 and HA-tagged Hsc70 in heat shock treated HEK cells; note that heat shock does not alter either TRPV1 or Hsc70 protein level. (b) Confocal images of HEK cells transfected with TRPV1-pHluorin or TRPV1-pHluorin + Hsc70 with or without heat shock treatment. Non permeabilized cells were immunostained with a GFP antibody (red) to detect TRPV1 at the cell surface. (c) Quantification of membrane versus total expression of TRPV1-pHluorin for different condition of heat shock treatment. Data are expressed as mean values \pm SEM ($n = 18$). *** $P < 0.001$. Two-way ANOVA followed by Tukey post test.

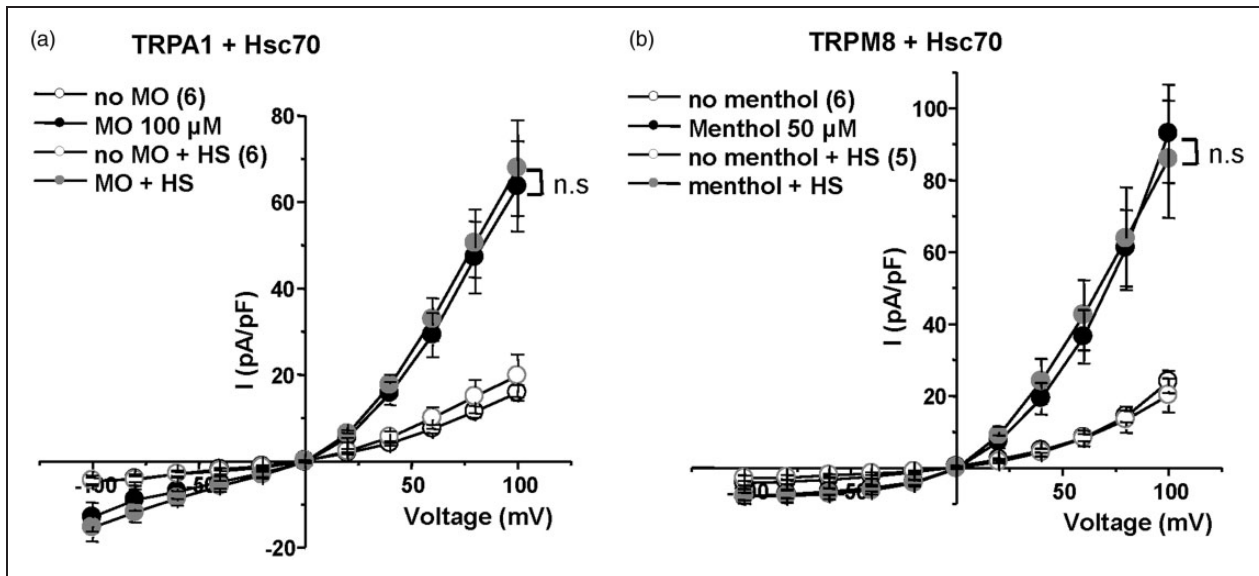


Figure 7. Hsc70-mediated current inhibition upon heat shock is specific to TRPV1 channel. (a) I–V curves of MO (100 μM)-evoked TRPA1 current in HEK cells cotransfected with TRPA1 and Hsc70 upon heat shock treatment. (b) Menthol (50 μM)-evoked TRPM8 current in HEK cells cotransfected with TRPM8 and Hsc70 upon heat shock treatment.

Surprisingly, in contrast to our findings with the capsaicin-activated TRPV1 channel, both TRPA1 and TRPM8, activated by mustard oil (100 μM) and menthol (50 μM), respectively, were insensitive to heat shock treatment (Figure 7(a) and (b)).

Hsc70-mediated heat shock inhibition of TRPV1 channels depends on ATP-ADP ratio

We then focused on determining the signaling elements involved in Hsc70-mediated inhibition of TRPV1. Because Hsc70 is an ATPase, we explored the possibility that altering the ATP–ADP cell content can prevent or mimic the Hsc70-mediated inhibitory effect. When ATP-bound, Hsc70 exhibits low affinity and quick exchange rates for its substrates, and the amount of Hsc70 oligomers is reduced in the presence of ATP.⁹ In contrast, the ADP-bound form has high affinity and slow exchange rates.^{1,10,11} Changing the ratio of ATP/ADP in the cell by adding either 2 mM ADP or ATP to the internal solution did not alter the capsaicin-induced current in cells transfected with TRPV1 alone (Figure 8). However, complete substitution of ATP with ADP led to a decrease in the capsaicin-induced TRPV1 peak current (obtained at +100 mV) in TRPV1/Hsc70 co-transfected cells (129.74 ± 9.71 to 52.18 ± 12.46 pA/pF; Figure 8(a) and (c)) or DRG neurons (107.86 ± 24.92 to 31.04 ± 7.33 pA/pF; Figure 8(b) and (c)). Altogether, these results indicate that cell stress prompts a transition into ADP-bound Hsc70, which leads to TRPV1 channel removal from the plasma membrane.

Hsc70-mediated heat shock inhibition of TRPV1 channels involves ROCK activation

Several cytoplasmic kinases are involved in modulating TRPV1 channel activity and trafficking,¹⁴ including PKC, MAPK, and Src Kinases.^{32,33} In attempting to delineate the effectors of Hsc70 signaling, we found that neither the broad PKC blocker GFX nor the MAP Kinase inhibitor U0126 were able to prevent nor to mimic Hsc70-mediated heat shock inhibition of TRPV1 in HEK cells (Figure 9). In contrast, application of the Rho-associated protein kinase (ROCK) inhibitor Y27362 mimicked the inhibitory effect on the capsaicin-induced current seen with heat shock, but only when Hsc70 was co-expressed with the channel. Based on these results, we hypothesized that, in response to heat shock, an Hsc70-mediated ROCK inhibition could in turn reduce TRPV1 surface expression at the plasma membrane.

Rho-kinase is a serine/threonine kinase belonging to the AGC family of protein kinases. The consensus sequence of the ROCK phosphorylation site is RXXS/T or RXS/T.³⁴ We found several ROCK phosphorylation sites in the sequence of TRPV1 including the S502 and S800 sites known to be involved in functional sensitization of the TRPV1 channel.³⁵ Testing Hsc70-mediated inhibition using TRPV1 channels mutated at these sites shows that the S502A mutant, but not the S800G or the WT channel, was unresponsive to heat shock in Hsc70-expressing cells (Figure 10(a)). Importantly, similar results were obtained in cells treated

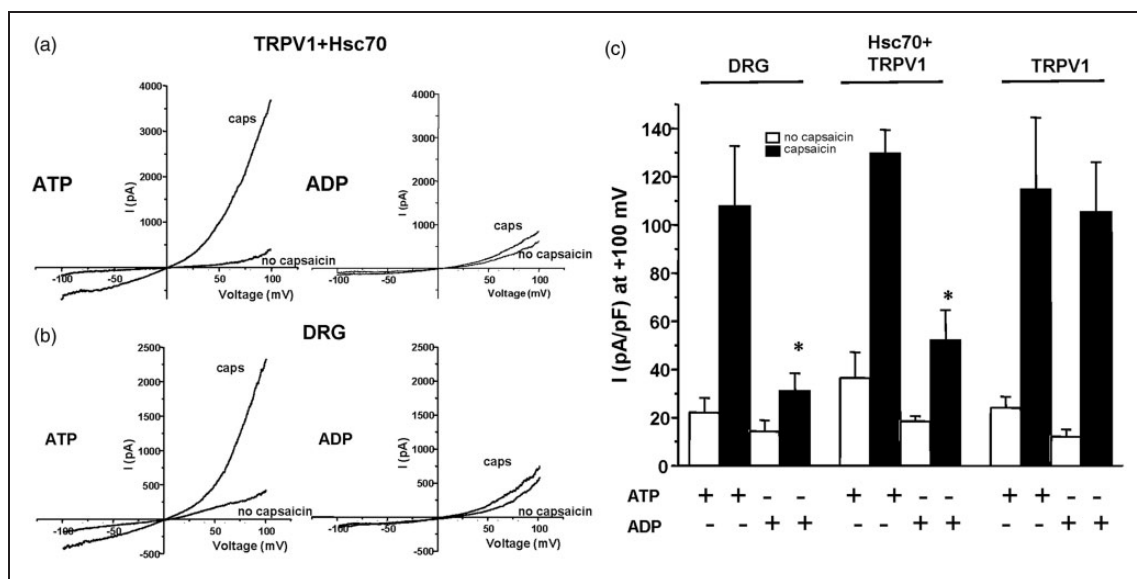


Figure 8. ADP-bound Hsc70 mediates channel inhibition. (a) TRPV1 current in transfected HEK cells elicited by a ramp protocol from -100 to $+100$ mV upon application of capsaicin (100 nM) in the presence of either 2 mM ATP or 2 mM ADP in the pipette solution. (b) TRPV1 current, in DRG neurons, elicited by a ramp protocol from -100 to $+100$ mV upon application of capsaicin (100 nM) in the presence of either 2 mM ATP or 2 mM ADP in the pipette solution. (c) peak of TRPV1 current density at $+100$ mV for different experimental conditions shown in (a) and (b). $*P < 0.05$. Paired t test.

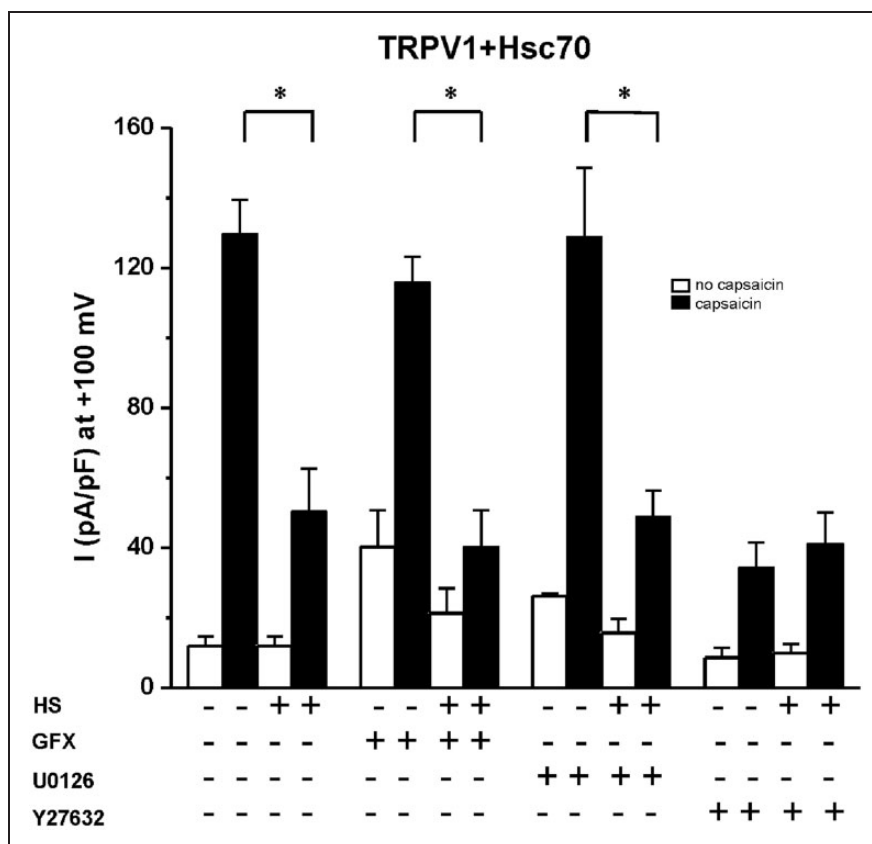


Figure 9. Hsc70-mediated decrease in TRPV1 current is independent of PKC or MAPK but acts through ROCK inhibition. Peak of TRPV1 current density at $+100$ mV measured in HEK cells transfected with TRPV1 + Hsc70 upon application of inhibitors of PKC (bisindolylmaleimide, GFX), MAPK (UO126), or ROCK (Y27632). Data are expressed as mean values \pm SEM ($n = 6$ to 8 cells per group). $*P < 0.05$.

with Y27362 in absence of heat shock, demonstrating that the heat shock-induced inhibition was mediated by blocking ROCK-dependent phosphorylation of TRPV1 subunit at the S502 site. Accordingly, measure of ROCK2 autophosphorylation from transfected HEK cells revealed that heat shock blocks ROCK activity in an Hsc70 dependent manner. Heat shock induced a minor reduction in phospho-ROCK2 from cells transfected with Hsc70 alone or TRPV1 alone. However, we found a pronounced decrease in ROCK2 autophosphorylation in HEK cells expressing both TRPV1 and Hsc70 (Figure 10(b) and (c)). Altogether, these results demonstrate that heat shock induces an Hsc70-mediated inactivation of ROCK, which in turn prevents the TRPV1 phosphorylation at residue S502 that leads to channel removal from the cell surface.

Discussion

We report the first evidence of HSP-mediated modulation of the nociceptive TRPV1 channel during the cell stress response. Expressed in dorsal root and trigeminal ganglia neurons, TRPV1 channels sense physical and chemical biohazards. In addition to transducing painful stimuli, TRPV1 signaling has been shown to mediate neuronal cell injury,³⁶ calcium toxicity,³⁷ and skeletal muscle hypertrophy highlighting the contribution of this channel to the cell stress response. Hsc70 is a molecular chaperone with diverse functions, including maintenance of protein homeostasis, cell survival, and autophagy.^{1,28} Hsc70 was found to protect neuroepithelial cells, neural precursor cells, and neurons from apoptosis during cell stress.³⁸⁻⁴¹ Moreover, Hsc70 promotes neuroregeneration and repair following cerebral ischemia, thus suggesting a neuroprotective role of this chaperone. While stress-inducible synthesis of HSPs (i.e. Hsp70) has been widely studied in both neural and non-neural tissue, the constitutively expressed Hsc70 is enriched in the mammalian nervous system, where thermal stress induces a translocation of Hsc70 at synaptic sites to control synaptic function.⁴² Importantly, recent findings demonstrated that drosophila Hsc70-4 is one of the most abundant synaptic proteins. Upon ATP-dependent oligomerization, the Hsc70-4 chaperone is able to deform synaptic membranes, a process required for microautophagy, thus promoting synaptic protein turnover. Consequently, loss of function of the chaperone was found to impair synaptic transmission.⁹ Here, we report an upregulation of Hsc70 expression level in lumbar DRGs from hyperalgesic CFA mice. In light of our data and previous findings, we suggest a functional link between TRPV1 and Hsc70 protein. Indeed, in response to inflammatory agents, such as bradykinin or NGF, TRPV1 trafficking is enhanced via a process that requires VAMP1-containing vesicle fusion mediated by

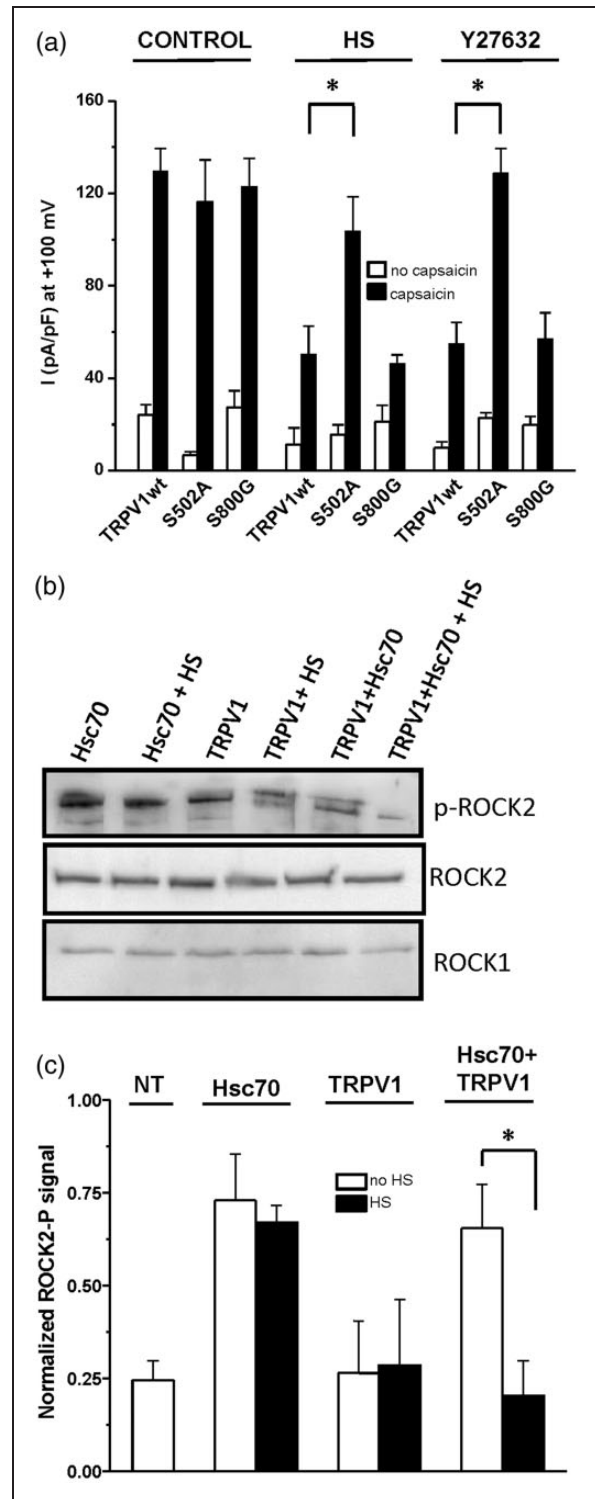


Figure 10. Hsc70-dependent inhibition of ROCK phosphorylation on TRPV1 S502 site. (a) Capsaicin-evoked peak current (at +100 mV) in HEK cells transfected with Hsc70 and each of the following: TRPV1 wt ($n = 6$), S502A ($n = 6$), and S800G ($n = 5$) mutant, in the absence and presence of heat shock and in the presence of the ROCK inhibitor Y27632 (10 μ M). (b) Representative WB showing the changes, after heat shock, in levels of phosphorylated ROCK (top), ROCK2 (middle) and ROCK1

(continued)

SNARE proteins (SNAP-25, VAMP1, and syntaxin1).⁴³ Importantly, the Hsc70-containing chaperone complex can biochemically interact with SNARE proteins to maintain them in an active state and promote vesicle fusion.⁴⁴ By examining the regulation of TRPV1 by Hsc70 during the cell stress response, we have discovered a functional relationship between Hsc70 and TRPV1 and show that Hsc70 can regulate TRPV1 trafficking possibly through its interaction with the SNARE complex. Our findings show that heat shock triggers a decrease in TRPV1 current, an effect that was suppressed by pharmacological blockers of Hsc70 in DRG neurons, and necessitates overexpression of the chaperone in transfected cells. Given that TRPV1 channels are activated by temperature,⁴⁵ we sought to determine whether Hsc70 expression would shift the temperature threshold of the channel, thus mediating channel desensitization in response to heat shock. Unexpectedly, we found that the conductance–temperature relationship of TRPV1 was not altered in the presence of Hsc70. Along these lines, the capsaicin dose-response curves did not indicate a decrease in capsaicin sensitivity, following heat shock challenge, and the gating properties of the channel were not affected.

Hsc70 is a pivotal cofactor that drives ubiquitination and degradation of numerous cellular proteins.¹ Overexpression of Hsc70 in *Xenopus* oocytes has been previously shown to increase the internalization of membrane bound epithelial sodium channels (ENaC), thereby inhibiting the sodium current.⁴ Using a TRPV1 channel bearing an extracellular GFP pHluorin, we measured a decrease in the amount of TRPV1 channels inserted into the plasma membrane after heat shock, but only in conditions of Hsc70 overexpression. Together with our Western blot analysis in Figure 6, these results indicate that thermal stress promotes a removal of membrane-bound TRPV1 channels through a process that requires Hsc70. Because we were not able to detect a physical interaction between Hsc70 and TRPV1 by co-immunoprecipitation (data not shown), we looked for an indirect Hsc70-mediated signaling implicated in TRPV1 current inhibition. The fact that Hsc70 activity and conformational change are regulated by ATP is well-documented.^{1,46} While ADP-bound Hsc70 exhibits high affinity and low exchange rates for the substrates, the ATP-bound form shows the opposite.^{1,46} By replacing ATP

with ADP in the internal solution of recording electrodes, we were able to replicate the decrease in capsaicin-evoked TRPV1 current even in the absence of heat shock. Based on this observation, we believe that saturating intracellular ADP produces a similar effect as the heat shock-driven rightward shift in the ATP/ADP-bound form of Hsc70. Given that ATP is able to promote chaperone activity by reducing Hsc70 oligomerization,^{5,9} we propose that heat shock-induced formation of Hsc70 oligomeric complexes prevents TRPV1 channel incorporation at the cell surface. Finally, our findings show that this inhibitory process is regulated by ROCK activity. Pharmacological inhibition of either the PKC or MAP kinase pathway did not alter heat shock modulation of TRPV1 current, whereas ROCK inhibition was able to mimic it in the presence of Hsc70. Phosphorylation of TRPV1 is a hallmark of channel sensitization that leads to pain hypersensitivity.¹⁴ Two major PKC-associated phosphorylation residues have been identified (S502 and S800), of the two, the S800 site seems to be a polymodal sensitization site that promotes PKC-induced hyperalgesia in an inflammatory setting.³⁵ Our results now show that inhibition of ROCK-dependent phosphorylation at the S502 site is crucial for mediating the heat shock effect, yet capsaicin dose response (data not shown) was not altered by blocking ROCK with Y27632. In support of this mechanism, phosphorylation of ROCK was suppressed in condition of heat shock but surprisingly only when both TRPV1 and Hsc70 were coexpressed. It is most likely that ROCK controls the trafficking of TRPV1 to the cell surface through a constitutive mechanism of phosphorylation at the TRPV1 S502 site. Upon heat shock, Hsc70-driven inhibition of ROCK might suppress TRPV1 channel incorporation at the cell surface, leading to less capsaicin-evoked current. While it is accepted that a balance of phosphorylation and dephosphorylation events regulate the activity and trafficking of a myriad of ion channels, our findings are the first to implicate ROCK in TRPV1 channel function, particularly in the context of cell stress response. Nevertheless, as TRPV1 is a polymodal sensor for heat, low pH, and lipids, it will be important to determine whether ROCK dependent phosphorylation controls other modalities of channel activation. In summary, we have shown that Hsc70 upregulation occurs in DRG neurons in response to inflammation and participates in the regulation of TRPV1 channel trafficking. The underlying mechanism involves an Hsc70-dependent inhibition of ROCK phosphorylation of TRPV1-S502 site. It will remain important to determine why Hsc70 is upregulated in DRGs during inflammation and whether it works as a protective mechanism to suppress inflammatory pain signals mediated by TRPV1 activation over time. Further work will be warranted to determine how such regulation

Figure 10. Continued

(bottom) in HEK cells expressing the indicated constructs ($n = 4$ independent experiments). (c) Densitometry analysis of phosphorylated-ROCK2 Western blot illustrated in (b). Note that a significant decrease in phosphorylated ROCK2 level appears only when HEK cells are cotransfected with TRPV1 + Hsc70 and treated with heat shock. * $P < 0.05$. Unpaired t test.

can be exploited to target TRPV1-driven pathogenesis, including neurogenic inflammation and inflammatory hypersensitivity. Moreover, this regulatory process is likely implicated in the context of cell survival and apoptosis during acute cell stress as well as other pathological processes that rely on Hsc70. Such processes could involve cancer, diabetes, or neurodegenerative diseases^{3,47} all of which have pain-associated pathology. Indeed, recent studies reported that TRPV1-deficient mice displayed greater metabolic health and longer life.⁴⁸ Given the importance of HSP in protein homeostasis and aging,⁴⁹ it is reasonable to postulate that the interplay between Hsc70 and TRPV1 may be implicated in metabolic health and hence the relationship between pain conditions and metabolic disturbances.

Acknowledgment

The authors thank Dr. Janice Braun for generously providing the mouse HA-tagged Hsc70 cDNA.

Declaration of Conflicting Interests

The author(s) declared no potential conflicts of interest with respect to the research, authorship, and/or publication of this article.

Funding

The author(s) disclosed receipt of the following financial support for the research, authorship, and/or publication of this article: This work was supported by operating grants from the Canadian Institutes of Health Research (CIHR) and by the Vi Riddell Child Pain program of the Alberta Children's Hospital Research Institute. CA holds a Canada Research Chair in inflammatory Pain (Tier2). LB holds an "Eyes High" fellowship from the University of Calgary.

References

- Liu T, Daniels CK and Cao S. Comprehensive review on the HSC70 functions, interactions with related molecules and involvement in clinical diseases and therapeutic potential. *Pharmacol Ther* 2012; 136: 354–374.
- Stricher F, Macri C, Ruff M, et al. HSPA8/HSC70 chaperone protein: structure, function, and chemical targeting. *Autophagy* 2013; 9: 1937–1954.
- Liao Y and Tang L. The critical roles of HSC70 in physiological and pathological processes. *Curr Pharm Des* 2014; 20: 101–107.
- Goldfarb SB, Kashlan OB, Watkins JN, et al. Differential effects of Hsc70 and Hsp70 on the intracellular trafficking and functional expression of epithelial sodium channels. *Proc Natl Acad Sci USA* 2006; 103: 5817–5822.
- Angelidis CE, Lazaridis I and Pagoulatos GN. Aggregation of hsp70 and hsc70 in vivo is distinct and temperature-dependent and their chaperone function is directly related to non-aggregated forms. *Eur J Biochem* 1999; 259: 505–512.
- Newmyer SL and Schmid SL. Dominant-interfering Hsc70 mutants disrupt multiple stages of the clathrin-coated vesicle cycle in vivo. *J Cell Biol* 2001; 152: 607–620.
- Bronk P, Wenniger JJ, Dawson-Scully K, et al. Drosophila Hsc70-4 is critical for neurotransmitter exocytosis in vivo. *Neuron* 2001; 30: 475–488.
- Sudhof TC and Rizo J. Synaptic vesicle exocytosis. *Cold Spring Harb Perspect Biol* 2011; 3: a005637.
- Uytterhoeven V, Lauwers E, Maes I, et al. Hsc70-4 deforms membranes to promote synaptic protein turnover by endosomal microautophagy. *Neuron* 2015; 88: 735–748.
- Benaroudj N, Triniolles F and Ladjimi MM. Effect of nucleotides, peptides, and unfolded proteins on the self-association of the molecular chaperone HSC70. *J Biol Chem* 1996; 271: 18471–18476.
- Gao B, Eisenberg E and Greene L. Effect of constitutive 70-kDa heat shock protein polymerization on its interaction with protein substrate. *J Biol Chem* 1996; 271: 16792–16797.
- Pratt WB, Gestwicki JE, Osawa Y, et al. Targeting Hsp90/Hsp70-based protein quality control for treatment of adult onset neurodegenerative diseases. *Annu Rev Pharmacol Toxicol* 2015; 55: 353–371.
- Vennekens R, Owsianik G and Nilius B. Vanilloid transient receptor potential cation channels: an overview. *Curr Pharm Des* 2008; 14: 18–31.
- Bourinet E, Altier C, Hildebrand ME, et al. Calcium-permeable ion channels in pain signaling. *Physiol Rev* 2014; 94: 81–140.
- Julius D. TRP channels and pain. *Annu Rev Cell Dev Biol* 2013; 29: 355–384.
- O'Neill J, Brock C, Olesen AE, et al. Unravelling the mystery of capsaicin: a tool to understand and treat pain. *Pharmacol Rev* 2012; 64: 939–971.
- Lapointe TK, Basso L, Iftinca MC, et al. TRPV1 sensitization mediates postinflammatory visceral pain following acute colitis. *Am J Physiol Gastrointest Liver Physiol* 2015; 309: G87–G99.
- Ruan T, Lin YS, Lin KS, et al. Sensory transduction of pulmonary reactive oxygen species by capsaicin-sensitive vagal lung afferent fibres in rats. *J Physiol* 2005; 565: 563–578.
- Nishio N, Taniguchi W, Sugimura YK, et al. Reactive oxygen species enhance excitatory synaptic transmission in rat spinal dorsal horn neurons by activating TRPA1 and TRPV1 channels. *Neuroscience* 2013; 247: 201–212.
- Weitlauf C, Ward NJ, Lambert WS, et al. Short-term increases in transient receptor potential vanilloid-1 mediate stress-induced enhancement of neuronal excitation. *J Neurosci* 2014; 34: 15369–15381.
- Kim SR, Kim SU, Oh U, et al. Transient receptor potential vanilloid subtype 1 mediates microglial cell death in vivo and in vitro via Ca²⁺-mediated mitochondrial damage and cytochrome c release. *J Immunol* 2006; 177: 4322–4329.
- Miller BA. The role of TRP channels in oxidative stress-induced cell death. *J Membr Biol* 2006; 209: 31–41.
- Dodson M, Darley-USmar V and Zhang J. Cellular metabolic and autophagic pathways: traffic control by redox signaling. *Free Radic Biol Med* 2013; 63: 207–221.

24. Tobaben S, Thakur P, Fernandez-Chacon R, et al. A trimeric protein complex functions as a synaptic chaperone machine. *Neuron* 2001; 31: 987–999.
25. Sharma M, Burre J and Sudhof TC. CSPalpha promotes SNARE-complex assembly by chaperoning SNAP-25 during synaptic activity. *Nat Cell Biol* 2011; 13: 30–39.
26. Nadler SG, Tepper MA, Schacter B, et al. Interaction of the immunosuppressant deoxyspergualin with a member of the Hsp70 family of heat shock proteins. *Science* 1992; 258: 484–486.
27. Mickle AD, Shepherd AJ, Loo L, et al. Induction of thermal and mechanical hypersensitivity by parathyroid hormone-related peptide through upregulation of TRPV1 function and trafficking. *Pain* 2015; 156: 1620–1636.
28. Holland S, Coste O, Zhang DD, et al. The ubiquitin ligase MYCBP2 regulates transient receptor potential vanilloid receptor 1 (TRPV1) internalization through inhibition of p38 MAPK signaling. *J Biol Chem* 2011; 286: 3671–3680.
29. Kang JH, Jiang Y, Toita R, et al. Phosphorylation of Rho-associated kinase (Rho-kinase/ROCK/ROK) substrates by protein kinases A and C. *Biochimie* 2007; 89: 39–47.
30. Wang S, Joseph J, Ro JY, et al. Modality-specific mechanisms of protein kinase C-induced hypersensitivity of TRPV1: S800 is a polymodal sensitization site. *Pain* 2015; 156: 931–941.
31. Song J, Lee JH, Lee SH, et al. TRPV1 activation in primary cortical neurons induces calcium-dependent programmed cell death. *Exp Neurol* 2013; 22: 51–57.
32. Ovey IS and Naziroglu M. Homocysteine and cytosolic GSH depletion induce apoptosis and oxidative toxicity through cytosolic calcium overload in the hippocampus of aged mice: involvement of TRPM2 and TRPV1 channels. *Neuroscience* 2015; 284: 225–233.
33. Rubio E, Valenciano AI, Segundo C, et al. Programmed cell death in the neurulating embryo is prevented by the chaperone heat shock cognate 70. *Eur J Neurosci* 2002; 15: 1646–1654.
34. Franklin TB, Krueger-Naug AM, Clarke DB, et al. The role of heat shock proteins Hsp70 and Hsp27 in cellular protection of the central nervous system. *Int J Hyperthermia* 2005; 21: 379–392.
35. Houenou LJ, Li L, Lei M, et al. Exogenous heat shock cognate protein Hsc 70 prevents axotomy-induced death of spinal sensory neurons. *Cell Stress Chaperones* 1996; 1: 161–166.
36. McLaughlin B, Hartnett KA, Erhardt JA, et al. Caspase 3 activation is essential for neuroprotection in preconditioning. *Proc Natl Acad Sci USA* 2003; 100: 715–720.
37. Chen S and Brown IR. Translocation of constitutively expressed heat shock protein Hsc70 to synapse-enriched areas of the cerebral cortex after hyperthermic stress. *J Neurosci Res* 2007; 85: 402–409.
38. Meng J, Wang J, Steinhoff M, et al. TNFalpha induces trafficking of TRPV1/TRPA1 in VAMP1-containing vesicles to the plasmalemma via Munc18-1/syntaxin1/SNAP-25 mediated fusion. *Sci Rep* 2016; 6: 21226.
39. Rizo J and Sudhof TC. The membrane fusion enigma: SNAREs, Sec1/Munc18 proteins, and their accomplices – guilty as charged? *Annu Rev Cell Dev Biol* 2012; 28: 279–308.
40. Voets T, Droogmans G, Wissenbach U, et al. The principle of temperature-dependent gating in cold- and heat-sensitive TRP channels. *Nature* 2004; 430: 748–754.
41. Yamagishi N, Ishihara K and Hatayama T. Hsp105alpha suppresses Hsc70 chaperone activity by inhibiting Hsc70 ATPase activity. *J Biol Chem* 2004; 279: 41727–41733.
42. Chen S and Brown IR. Neuronal expression of constitutive heat shock proteins: implications for neurodegenerative diseases. *Cell Stress Chaperones* 2007; 12: 51–58.
43. Riera CE, Huising MO, Follett P, et al. TRPV1 pain receptors regulate longevity and metabolism by neuropeptide signaling. *Cell* 2014; 157: 1023–1036.
44. Nillegoda NB, Kirstein J, Szlachetka A, et al. Crucial HSP70 co-chaperone complex unlocks metazoan protein disaggregation. *Nature* 2015; 524: 247–251.
45. Flynn R, Chapman K, Iftinca M, et al. Targeting the transient receptor potential vanilloid type 1 (TRPV1) assembly domain attenuates inflammation-induced hypersensitivity. *J Biol Chem* 2014; 289: 16675–16687.
46. Altier C, Garcia-Caballero A, Simms B, et al. The Cavbeta subunit prevents RFP2-mediated ubiquitination and proteasomal degradation of L-type channels. *Nat Neurosci* 2011; 14: 173–180.
47. Caterina MJ, Schumacher MA, Tominaga M, et al. The capsaicin receptor: a heat-activated ion channel in the pain pathway. *Nature* 1997; 389: 816–824.
48. Helliwell RJ, McLatchie LM, Clarke M, et al. Capsaicin sensitivity is associated with the expression of the vanilloid (capsaicin) receptor (VR1) mRNA in adult rat sensory ganglia. *Neurosci Lett* 1998; 250: 177–180.
49. Roberts JC, Davis JB and Benham CD. [3H]Resiniferatoxin autoradiography in the CNS of wild-type and TRPV1 null mice defines TRPV1 (VR-1) protein distribution. *Brain Res* 2004; 995: 176–183.